RESEARCH ARTICLE

CrossMark

The antioxidative defense system is involved in the premature senescence in transgenic tobacco (*Nicotiana tabacum NC89*)

Yu Liu[1], Lu Wang[1], Heng Liu[1], Rongrong Zhao[1], Bin Liu[1], Quanjuan Fu[2] and Yuanhu Zhang[1*]

Abstract

Background: α-Farnesene is a volatile sesquiterpene synthesized by the plant mevalonate (MVA) pathway through the action of α-farnesene synthase. The *α-farnesene synthase 1* (*MdAFS1*) gene was isolated from apple peel (var. *white winter pearmain*), and transformed into tobacco (*Nicotiana tabacum* NC89). The transgenic plants had faster stem elongation during vegetative growth and earlier flowering than wild type (WT). Our studies focused on the transgenic tobacco phenotype.

Results: The levels of chlorophyll and soluble protein decreased and a lower seed biomass and reduced net photosynthetic rate (Pn) in transgenic plants. Reactive oxygen species (ROS) such as hydrogen peroxide (H_2O_2) and superoxide radicals ($O_2^{\cdot-}$) had higher levels in transgenics compared to controls. Transgenic plants also had enhanced sensitivity to oxidative stress. The transcriptome of 8-week-old plants was studied to detect molecular changes. Differentially expressed unigene analysis showed that ubiquitin-mediated proteolysis, cell growth, and death unigenes were upregulated. Unigenes related to photosynthesis, antioxidant activity, and nitrogen metabolism were downregulated. Combined with the expression analysis of senescence marker genes, these results indicate that senescence started in the leaves of the transgenic plants at the vegetative growth stage.

Conclusions: The antioxidative defense system was compromised and the accumulation of reactive oxygen species (ROS) played an important role in the premature aging of transgenic plants.

Keywords: Tobacco, Senescence, Transcriptome, Reactive oxygen species (ROS)

Background

α-Farnesene is a volatile plant sesquiterpene. It also acts as a semiochemical that can affect the behavior of some insect species [1, 2]. α-Farnesene can accumulate in apple peel, and the oxidative production of α-farnesene is associated with the development of scald symptoms [3, 4], a physiological disorder of apple and pear fruits [5, 6]. α-Farnesene synthesis mainly occurs via the cytosolic mevalonic acid (MVA) pathway, which is initiated by the first rate-limiting enzyme, 3-hydroxy-3-methylglutaryl-CoA reductase (HMGR) [7]. The other important step

in the α-farnesene synthesis pathway involves farnesyl diphosphate synthase (FPS). FPS catalyzes the condensation of geranyl diphosphate (GPP) and isopentenyl diphosphate (IPP) to produce farnesyl diphosphate (FPP), which is the immediate precursor of sesquiterpenes [8]. In the final step of synthesis, α-farnesene synthase uses FPP as the substrate to catalyze the synthesis of α-farnesene. Pechous and Whitaker (2004) cloned the *α-farnesene synthase 1* (*AFS1*) gene of the 'Law Rome' apple and expressed it in bacteria [9]. When farnesyl diphosphate (FPP) was supplied as the substrate for the bacterially expressed recombinant enzyme, α-farnesene was synthesized.

Terpenoids play crucial roles in plant defense, growth, and development. Genetic engineering of key genes involved in the terpene synthesis pathway has generated

*Correspondence: yyhzhang@sdau.edu.cn
[1] State Key Laboratory of Crop Biology, College of Life Sciences, Shandong Agricultural University, 61 Dai Zong Street, Tai'an 271018, Shandong, People's Republic of China
Full list of author information is available at the end of the article

Liu *et al. Biol Res* (2016) 49:30

Page 2 of 15

mutants and transgenic plants with altered growth and development. For example, the *hmg1* mutant exhibits dwarfing, early senescence, sterility, and earlier induction of the *senescence-associated 12* (*SAG12*) gene compared to wild-type (WT) plants [10]. In *Arabidopsis thaliana*, farnesyl diphosphate synthase 1 (FPS1) and farnesyl diphosphate synthase 2 (FPS2), which encode cytosolic FDP synthase, are differentially expressed [11]. Compared to WT, overexpression of *A. thaliana FPS1* results in a cell death/senescence-like phenotype, which grew less vigorously than wild-type plants, and premature induction of the *SAG12* gene [12]. Overexpression of *A. thaliana FPS2* leads to the synthesis of several novel sesquiterpenes, including E-β-farnesene, and transgenic plants show enhanced growth [13]. Of the three functional FPPS in maize, *FPPS3* is induced by herbivory, and is essential to the production of the volatile sesquiterpenes, including β-caryophyllene [14]. Sesquiterpenes play an important role in plant physiological and ecological functions such as scavenging for reactive oxygen species (ROS), stabilizing membrane structure, and inhibiting bacterial growth [15, 16]. Treatment of *Aquilaria sinensis* (Lour.) cell culture suspensions with hydrogen peroxide (H_2O_2) induces the production of sesquiterpenes, stimulates programmed cell death (PCD), and increases salicylic acid (SA) accumulation. These results indicate potential interactions between sesquiterpene synthesis and programmed cell death (PCD) during *A. sinensis* (agarwood) formation [17]. In plants, terpenes are synthesized via the mevalonate (MVA) pathway in the cytosol and peroxisomes, and the 2-C-methyl-D-erythritol 4-P/1-deoxy-D-xylulose 5-P (MEP) pathway in plastids [18]. The two pathways are capable of exchanging intermediates [19]. In the MEP pathway, disruption of the *1-deoxy-D-xylulose-5-phosphate reductoisomerase* (*DXR*) gene leads to biosynthetic deficiency of photosynthetic pigments, GAs and ABA, resulting in developmental abnormalities [20]. Monoterpenes are volatile terpenes synthesized by the MEP pathway. Monoterpenes also play key roles in plant defense and apoptosis-like cell death [21–23].

Leaf senescence is characterized by degradation of the chlorophyll, photosynthetic proteins and other macromolecules, conversion of peroxisomes into glyoxysomes, and increased production of ROS [24]. ROS are a central element of the senescence process, which is toxic to plant cells [25]. Excessive production of ROS causes necrosis via programmed cell death [26]. The chloroplast is the most important organelle in $^1O_2$ production and is also regarded as the major intracellular producer of partially reduced oxygen species such as H_2O_2 and O_2^- [27]. Chloroplasts, which are a rich source of nitrogen (N), are the first organelles that are dismantled during senescence

[28]. Nutrient signaling also plays important roles in leaf senescence. For example, leaf senescence is induced when sugar levels exceed or decrease beyond acceptable threshold levels [29, 30]. Sugar-induced senescence is particularly important in conditions of low nitrogen availability and may also play a role in light signaling [31, 32].

Overexpression of *α-farnesene synthase 1* (*MdAFS1*) in transgenic tobacco plants has been associated with an unexpected phenotype, specifically accelerated stem elongation and early flowering, compared to WT plants. Therefore, in this study, transcriptome analysis of transgenic tobacco plants was conducted to study the differentially expressed genes. We concluded that the antioxidative defense system is compromised, and accumulation of ROS activates the senescence process. In the future, we anticipate that the transcriptome database will be a valuable resource for improved understanding of the molecular basis for alterations in plant growth and development.
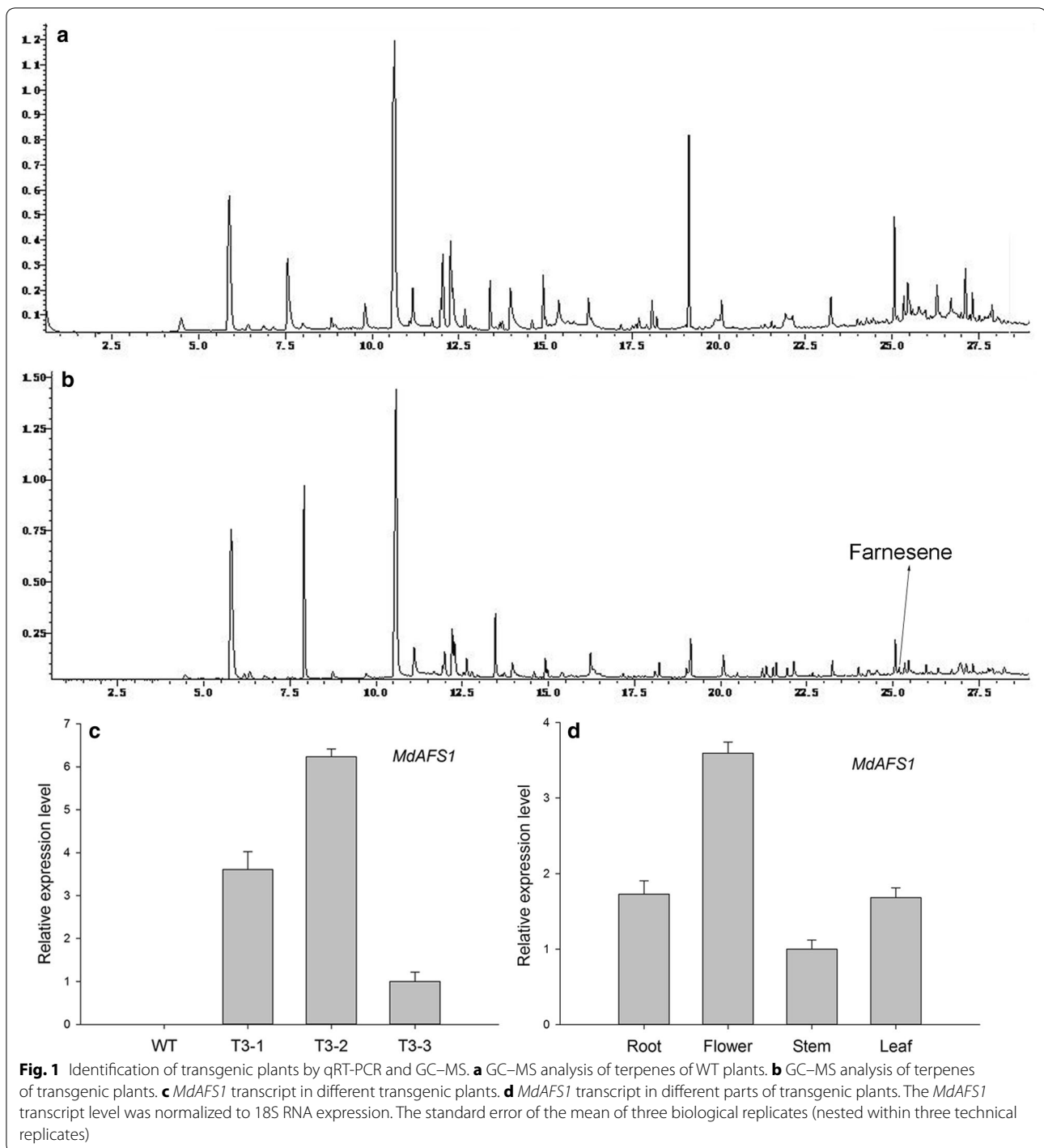
Results

Identification of transgenic plants

Three third generation lines were selected for identification of transgenic plants at the transcript level. The relative *MdAFS1* mRNA levels of the transgenic lines were average, higher, and lower in T3-1, T3-2 and T3-3, respectively (Fig. 1c). Expression levels of *MdAFS1* varied in different parts of the transgenic plants; it had a higher transcript level in the flowers (Fig. 1d). So, flowers were selected as experimental materials for GC–MS analysis of the terpenes. The release of farnesene (0.41 %) was detected in the flowers of transgenic plants (Fig. 1a, b). The chemical formula of farnesene is $C_{15}H_{24}$ and the molecular weight is 204. In addition to this, β-myrcene (0.34 %), linalool (5.92 %), and caryophyllene (2.98 %) were detected in WT plants. The release of linalool (2.3 %) and caryophyllene (1.71 %) was detected in the flowers of transgenic plants (Table 1).

Plant phenotype analysis

To determine growth differences in the WT, T3-1, T3-2 and T3-3, plant height, leaf area, and seed biomass were measured. At 8 weeks of age, the stem of transgenic plants had accelerated elongation with lengths reaching about 21 cm, whereas WT stems were approximately 2.0 cm in length (Fig. 2B). The transgenic plants flowered at about 10 weeks of age and had mature seeds at 18 weeks. At 18 weeks, the WT plants were still in full bloom. The heights of the tobacco plants were as follows: 108.0 cm, 81.7 cm, 84.0 cm and 83.3 cm for WT, T3-1, T3-2 and T3-3, respectively (Fig. 2C). Based on changes in height throughout the developmental process, the transgenic

Liu *et al. Biol Res* (2016) 49:30

Page 3 of 15

Fig. 1 Identification of transgenic plants by qRT-PCR and GC–MS. **a** GC–MS analysis of terpenes of WT plants. **b** GC–MS analysis of terpenes of transgenic plants. **c** *MdAFS1* transcript in different transgenic plants. **d** *MdAFS1* transcript in different parts of transgenic plants. The *MdAFS1* transcript level was normalized to 18S RNA expression. The standard error of the mean of three biological replicates (nested within three technical replicates)

plants had faster development (Fig. 2A). At 8 weeks old, the transgenic plants showed no change in leaf biomass, a fivefold increase in stem biomass, and a twofold increase in root biomass (Table 2). There were 9–10 leaves per transgenic plant, whereas WT plants had 8 leaves. Leaf area was measured at different locations on transgenic and WT plants. Transgenic plants showed no changes in total

leaf area but the functional leaf area significantly decreased and the upper leaf area significantly increased (Table 3).

The transgenic plants have reduced seed biomass

Seed biomass was considered an important indicator of reproductive growth. One capsule of tobacco (*NC89*) contains 1500–2000 grains. Though the weight per 1000

Liu *et al. Biol Res* (2016) 49:30

Page 4 of 15

Table 1 GC-MS analysis of tobacco terpenes

Retention time (min)	Compound formula	Compound name	Relative percentage content (%)	
			WT	T3-2
16.317	$C_{10}H_{16}$	β-Myrcene	0.34	–
19.127	$C_{10}H_{16}$	Linalool	5.92	2.3
25.064	$C_{15}H_{24}$	Caryophyllene	2.98	1.71
25.175	$C_{15}H_{24}$	Farnesene	–	0.41

"–" Indicates that this compound was not tested

grains increased by 117.1, 115.6 and 111.4 %, the number of capsules decreased by 66.7, 70.8 and 76.9 % in the T3-1, T3-2, and T3-3 lines, respectively, compared to WT plants (Table 4). Given these results, the transgenic plants produced less seed biomass than WT plants.

Physiological parameters related to senescence

Leaf senescence generally accelerates chlorophyll degradation and cell death [33, 34], which occur simultaneously with protein degradation. For these reasons, chlorophyll and soluble protein levels were measured. The T3-1, T3-2 and T3-3 plants showed a decrease in the content of chlorophyll *a* by 87.1, 83.9 and 78.2 %;
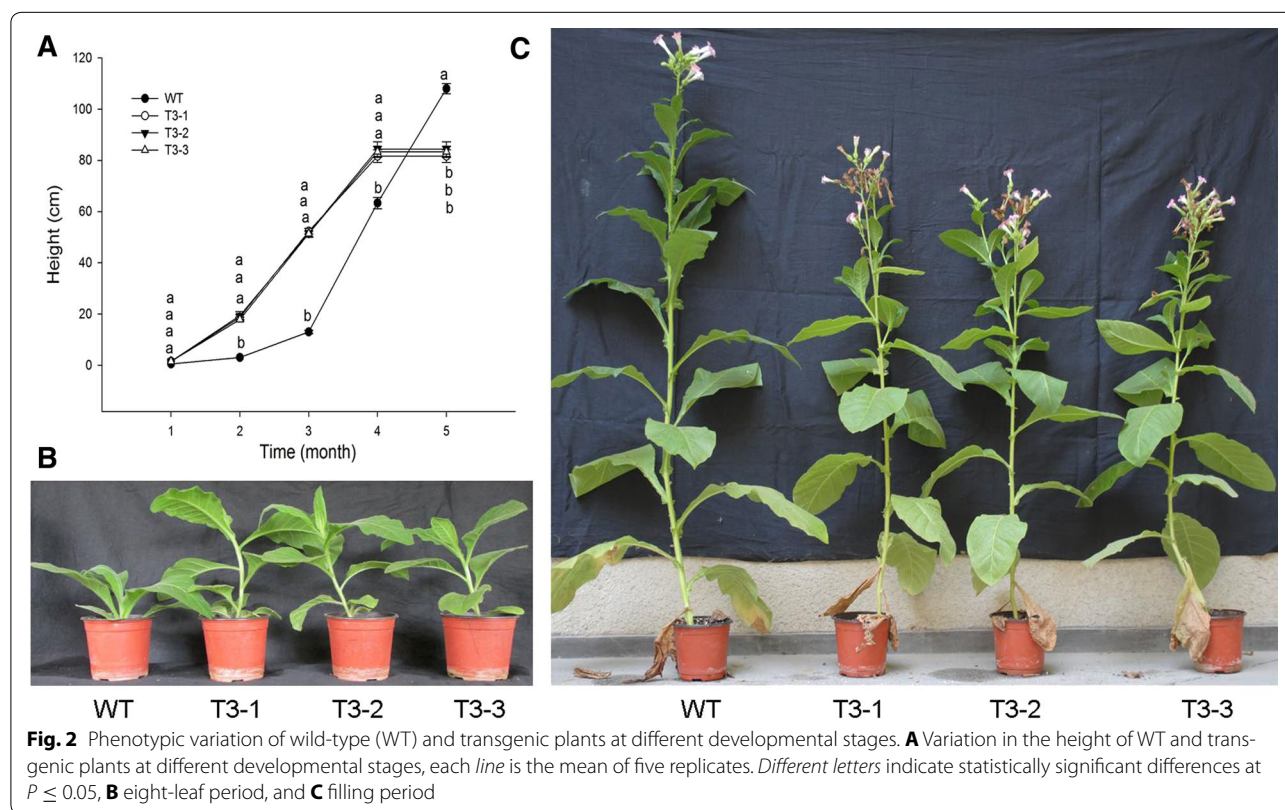
Fig. 2 Phenotypic variation of wild-type (WT) and transgenic plants at different developmental stages. **A** Variation in the height of WT and transgenic plants at different developmental stages, each *line* is the mean of five replicates. *Different letters* indicate statistically significant differences at $P \leq 0.05$, **B** eight-leaf period, and **C** filling period

Table 2 Biomass of tissues from wild-type (WT) and transgenic (T) plants

Biomass (g)	WT	T3-1	T3-2	T3-3
Root	1.73 ± 0.09b	3.26 ± 0.62a	3.06 ± 0.10a	3.65 ± 0.76a
Stem	2.19 ± 0.09b	10.84 ± 1.90a	10.76 ± 0.63a	11.46 ± 1.90a
Leaf	21.33 ± 4.33a	20.93 ± 2.82a	20.63 ± 1.52a	22.57 ± 2.61a
Total	25.25 ± 2.70b	35.03 ± 12.90a	34.46 ± 4.60a	37.67 ± 17.53a

Each line represents the mean of five replicates. *Different letters* indicate statistically significant differences at $P \leq 0.05$ in same parts of wild-type (WT) and transgenic (T) plants

Liu *et al. Biol Res (2016) 49:30*

Page 5 of 15

Table 3 Leaf area of WT and transgenic (T) plants

Lines	1 (cm²)	2 (cm²)	3 (cm²)	4 (cm²)	5 (cm²)	6 (cm²)	7 (cm²)	8 (cm²)	9 (cm²)
WT	28.8 ± 5.0a	62.8 ± 13.3a	82.9 ± 14.7a	158.5 ± 14.6a	154.8 ± 12.4a	112.8 ± 5.4a	77.9 ± 8.9a	25.3 ± 7.6b	
T3-1	26 ± 8.4a	59.2 ± 21.0a	97.3 ± 4.8a	96.8 ± 1.1b	132.9 ± 2.6b	103.0 ± 6.5a	89.5 ± 7.0a	56.4 ± 14.2a	18.7 ± 6.5
T3-2	30.2 ± 1.0a	67.5 ± 2.7a	89.9 ± 10.2a	124.6 ± 5.6b	133.5 ± 2.7b	111.4 ± 12.0a	86.1 ± 11.6a	53.2 ± 0.3ab	23.2 ± 2.9
T3-3	24.8 ± 3.2a	58.0 ± 8.4a	81.4 ± 1.9a	116.7 ± 11.9b	128.9 ± 6.7b	116.1 ± 1.5a	88.8 ± 6.2a	53.5 ± 10.5ab	31.1 ± 16.3

Each line represents a mean of five replicates. *Different letters* indicate statistically significant differences at $P \leq 0.05$ in same leaf position of wild-type (WT) and transgenic (T) plants

Table 4 Seed biomass of WT and transgenic (T) tobacco plants

Biomass	WT	T3-1	T3-2	T3-3
Capsule (number)	24.0 ± 1.0a	16.0 ± 1.0b	17.0 ± 3.0b	16.3 ± 2.3b
Weight per 1000 grains (mg)	76.2 ± 1.5c	89.2 ± 3.5a	88.1 ± 1.8a	84.9 ± 2.2b

Tobacco seeds dried to constant weight were used in this experiment. Values shown are means ± SE (five biological replicates is presented)

Different letters indicate statistically significant differences at $P \leq 0.05$

chlorophyll *b* decreased by 93.7, 86.3 and 80.4 %; the total chlorophyll (a + b) content decreased by 88.2, 88.3 and 84 % (Fig. 3A) and carotenoid content decreased by 70.5, 79.2 and 73.9 %, respectively (Fig. 3B). Soluble protein levels decreased significantly, by 53.8, 51.6 and 53.3 % in T3-1, T3-2 and T3-3, respectively (Fig. 3C). Chlorophyll and photosynthesis proteins are important elements in photosynthesis. The value of Pn decreased significantly by 82.7, 81.9 and 84.8 % in three transgenic lines (Fig. 3D). Water content showed a significant reduction (Fig. 3E). Malondialdehyde (MDA) is the decomposition product of membrane lipid peroxidation, and it accumulates in senescent leaves. MDA content increased by 121.7, 127.1 and 119.7 % in the T3-1, T3-2, and T3-3 lines, respectively (Fig. 3F).

Differentially expressed unigenes in leaf transcriptome data are related to senescence

The molecular mechanism underlying leaf senescence in transgenic tobacco was studied using transcriptome analysis of 8-week-old plants. De novo transcriptome assembly generated a total of 249,185 unigenes. The total number of differentially expressed transcripts ($P \leq 0.01$, ratio ≥ 2 or ≤ 0.5) was 5835, of which 2028 were upregulated and 3807 were downregulated in transgenic plants. The expression levels of six differentially expressed unigenes and three antioxidant enzyme genes were analyzed using qRT-PCR to test the reliability of the transcriptome database. The results were consistent with the transcriptome data (Additional file 1: Fig. S1). To classify the predicted functions of the unigenes, nucleotide and protein databases were used. GO and KEGG analyses

showed that some differentially expressed unigenes were related to leaf senescence. For example, ubiquitin-mediated proteolysis, cell growth, and death were upregulated unigenes. However, antioxidant enzymes, nitrogen metabolism, photosynthesis, and carotenoid biosynthesis were downregulated unigenes (Additional files 2, 3). A total of 87 downregulated unigenes of the photosynthesis signaling pathway are presented in Fig. 4. All transcripts of tobacco (*N. tabacum* NC89) have been deposited to GenBank as Accession Number GDGU00000000.

### Accumulation of reactive oxygen species (ROS) in transgenic plants

As indicators of oxidative stress and leaf senescence, the levels of $O_2^{\cdot-}$ and H_2O_2 in leaf tissues were measured under controlled conditions. Transgenic plants, T3-1, T3-2 and T3-3, had increases in the production rate of $O_2^{\cdot-}$ by 138.0, 147.5 and 136.6 % (Fig. 5A), and H_2O_2 levels increased by 111.5, 115.3 and 119.8 %, respectively (Fig. 5B). Histochemical staining can detect the accumulation of reactive oxygen species (ROS); deeper 3,3′-diaminobenzidine (DAB) and nitroblue tetrazolium (NBT) staining was seen in transgenic plants. These findings were consistent with the ROS content results.

Antioxidant enzyme activity and gene expression analysis

Antioxidant enzymes participated in the scavenging of ROS. However, the activity of three antioxidant enzymes in T3-1, T3-2 and T3-3 decreased significantly, APX by 52.6, 42.9 and 43.4 %; CAT by 63.7, 56.6 and 65.3 %; and SOD by 59.1, 46.4 and 44.7 %, respectively (Fig. 6). The expression of antioxidant enzyme genes were consistent with the enzyme activity, which were downregulated in transgenic plants.

Enhanced sensitivity of transgenic plants to DCMU treatment

The 3-(3,4-dichlorfenyl)-1,1-dimethylkarbonyldiamid (DCMU) molecule is an electron transfer inhibitor that acts during photosynthesis. Exogenous DCMU treatment induces production of ROS in the chloroplasts. Three week old plants were treated with 70 µM DCMU. After 10 days, all the transgenic plants had died, but the WT plants were

Liu *et al. Biol Res* (2016) 49:30

Page 6 of 15
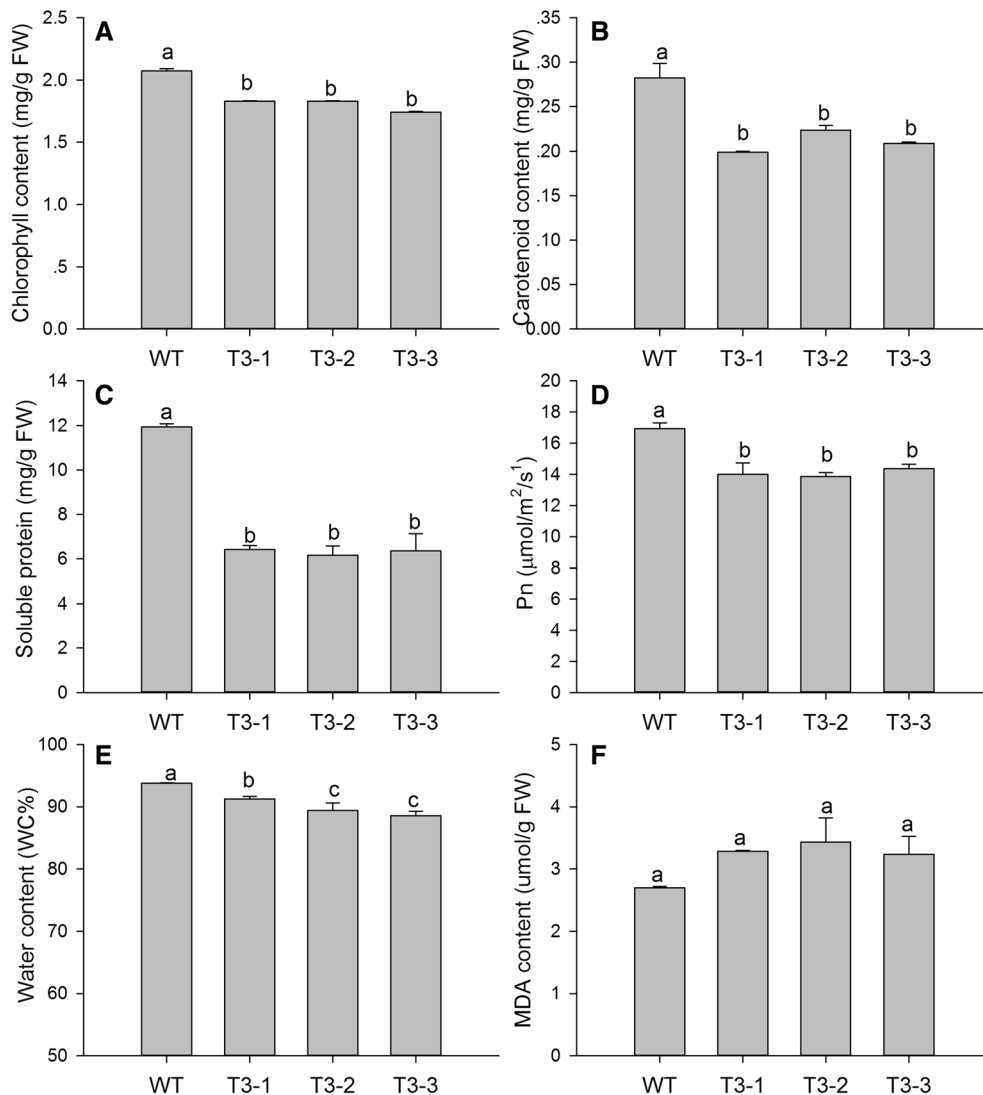
Fig. 3 Measurement of senescence-related physiological parameters in WT and transgenic plants. **A** Chlorophyll content, **B** carotenoid content, **C** soluble protein content, **D** net photosynthetic rate, **E** shows water content, and **F** signifies malondialdehyde (MDA) content. Data are mean ± SE (n = 5, five biological replicates per *line*). *Different letters* indicate statistically significant differences at $P \leq 0.05$

still alive (Fig. 7). This result indicated that the transgenic plants were more sensitive to oxidative stress.
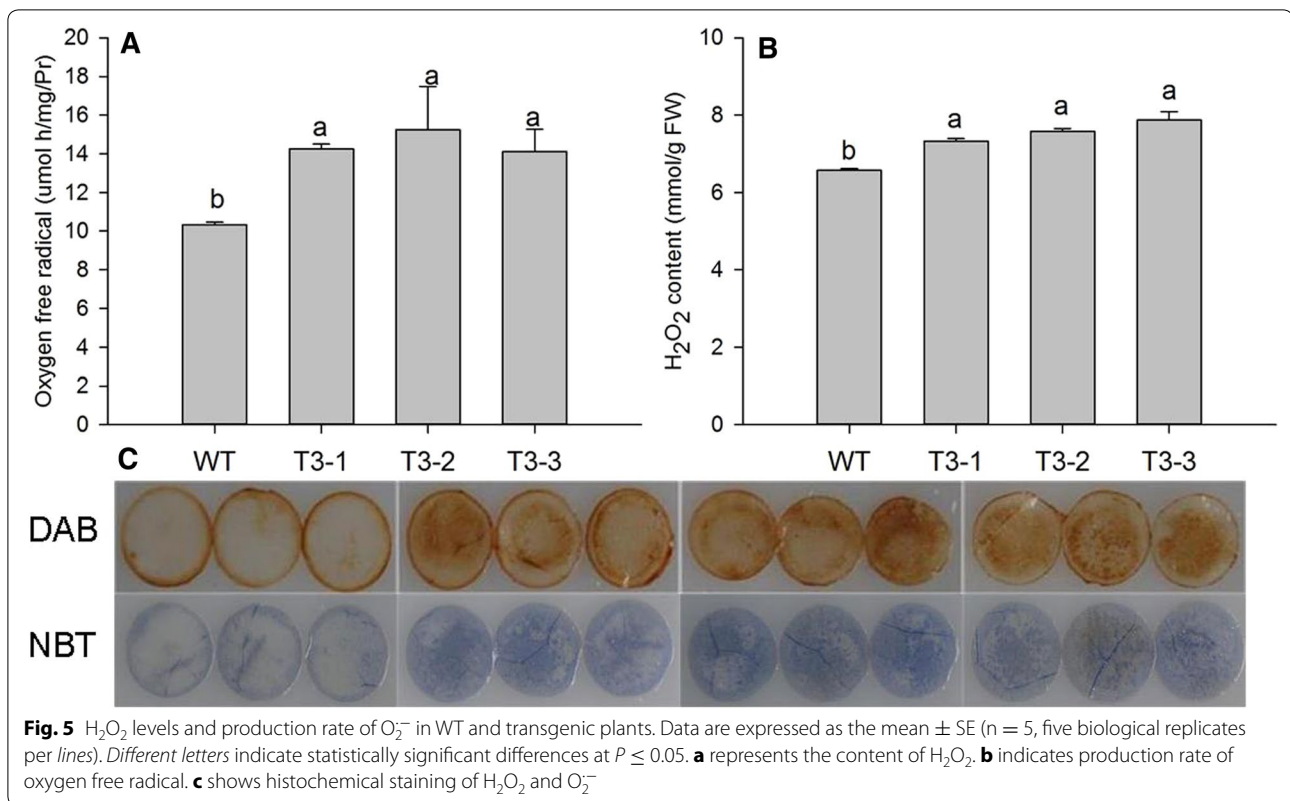
Expression of senescence marker genes

Based on the leaf senescence database (LSD, http://www.eplantsenescence.org/) and the typical characteristics of leaf senescence, senescence-related downregulated genes were selected, including chlorophyll *a/b* binding protein (*CAB*), ribulose-1,5-bisphosphate carboxylase-oxygenase small subunit (*RBCS2B*), nitrate reductase (*Nia*), and chloroplastic glutamine synthetase (*GS2*). The upregulated genes included cysteine proteinase (*NtCP1* and *SAG12*), glutamate dehydrogenase (*GDH*),

chlorophyllase (*CHL*), and *Ntdin*. qRT-PCR confirmed that *CAB*, *RBCS2B*, *Nia*, and *GS2* were downregulated and that *NtCP1*, *SAG12*, *GDH*, *CHL*, and *Ntdin* were upregulated (Fig. 8). The transcript levels of these senescence marker genes are consistent with the premature senescence characteristic.

Discussion

Transgenic plants showed a distinct premature senescence phenotype. The stems of transgenic plants rapidly elongated compared to those of WT plants. This occurred during the 7 week interval between first true leaf appearance to emergence of flower primordia (Fig. 2A).

Liu *et al. Biol Res* (2016) 49:30

Page 7 of 15

Fig. 4 Kyoto encyclopedia of genes and genomes (KEGG) pathway analysis of photosynthesis. *Green* represents downregulated unigenes ($P \leq 0.01$, ratio ≤ 0.5). *psbS* chloroplast photosystem II 22 kDa component, *psaN* photosystem I reaction center subunit, *psbY* photosystem II core complex proteins, *psbP* photosystem II oxygen-evolving enhancer protein 2, *petC* Rieske FeS precursor protein 2, *atpG* gamma subunit of ATP synthase, *petE* plastocyanin A, *psb27* photosystem II Psb27 protein, *psbO* chloroplast PsbO4 precursor, *psaH* photosystem I reaction centre subunit, *psaG* photosystem I reaction center V, *petF* ferredoxin, *atpF* ATP synthase subunit b, *psbW* photosystem II PsbW protein, *petH* ferredoxin-NADP reductase, *psbQ* photosystem II oxygen-evolving enhancer protein 3, *psbR* photosystem II 10 kDa polypeptide, *psbA* photosystem II protein D1

Transgenics had early flowering at about 50 days which was associated with a shorter vegetative period. Tobacco plants exhibited successive leaf senescence, starting from the basal leaves and advancing toward the apical leaves. At the filling period, which generally occurs in 20 week-old plants, the T3-1, T3-2 and T3-3 plants had at least two dead basal leaves, whereas WT plants only had one dead basal leaf (Fig. 2C). Changes in transgenic plant phenotype were indicative of premature senescence. Meanwhile, the transgenic plants developed new stems at the upper part of the plant. This phenomenon might be related to weak sink strength, which causes a slower progression of senescence in tobacco [35]. The new collateral delayed the death of the whole plant. Tobacco senescence is largely independent of floral development making it a model plant species for research [36]. However, leaf senescence in transgenic plants began during vegetative growth.

The main physiological purpose of leaf senescence is nutrient salvage involving the hydrolysis of macromolecules and their subsequent remobilization to other plant parts [37, 38]. We speculated that transgenic tobacco leaves activated the nutrient salvage program. Carbohydrates were temporarily stored in the stem and root tissues during vegetative growth, resulting in an increase the biomass of stems and roots (Table 2). This allocation of nutrients is beneficial to carbohydrate reserves and to the reduction of energy consumption [39], thereby remobilizing reproductive growth [28, 40]. At the reproductive stage, the premature senescent leaves of transgenic plants appeared to remobilize nutrients to the limited number of seeds, and increased the weight per 1000 grains. However, the decrease in total seed biomass is the result of senescence of transgenic plants.

Leaf senescence can be triggered by high C:N ratios [41, 42]. Glucose and sucrose repress the transcription

Liu *et al. Biol Res* (2016) 49:30

Page 8 of 15

Fig. 5 H_2O_2 levels and production rate of $O_2^{\cdot-}$ in WT and transgenic plants. Data are expressed as the mean ± SE (n = 5, five biological replicates per *lines*). *Different letters* indicate statistically significant differences at $P \leq 0.05$. **a** represents the content of H_2O_2. **b** indicates production rate of oxygen free radical. **c** shows histochemical staining of H_2O_2 and $O_2^{\cdot-}$

of photosynthetic genes, probably via *hexokinase*, which acts as a sugar sensor, and by sugar phosphorylation, which mediates carbohydrate signal transduction [43]. Overexpression of *Arabidopsis hexokinase* in tomato plants induces rapid senescence [44]. In contrast, antisense or *hexokinase* mutants exhibit a delayed senescence phenotype, suggesting that *hexokinase* is involved in senescence regulation [45]. In the present study, *hexokinase* is an upregulated unigene, which is likely to be involved with inducing senescence. In nitrogen metabolism, 62 transcripts were downregulated (Additional file 2). The expression of genes involved in primary nitrogen assimilation such as *GS2* (chloroplastic glutamine synthetase) and *Nia* (nitrate reductase) were repressed; in contrast, *GDH* (glutamate dehydrogenase) mRNA accumulation was increased (Fig. 8). This suggests that primary nitrogen assimilation was suppressed, and nitrogen remobilization was activated in transgenic plants. After treatment of tobacco leaf discs with hydrogen peroxide (H_2O_2) GDH mRNA accumulated, and GS2 mRNA decreased [46]. So the expression of GDH and GS2 also suggests the accumulation of ROS in transgenic plants. In addition, nitrogen is major element of soluble protein. Soluble protein degradation was indicative of lower nitrogen content (Fig. 3C).

Leaf senescence occurs during oxidative stress, which can be induced by overproduction of ROS [47]. Plants cope with oxidative stress using antioxidative systems including antioxidative enzymes such as glutathione peroxidases, dehydroascorbate reductase, catalase (CAT), superoxide dismutase (SOD), and ascorbate peroxidase (APX), and antioxidative metabolites such as ascorbate, glutathione, tocopherol, and carotenoids [48, 49]. In our study, the lower carotenoids, polyphenols, and flavonoid level could weaken their recognized roles in protecting photosystems from oxidative stress (Fig. 3B; Additional file 4: Fig. S2). Because SOD is responsible for dismutation of $O_2^{\cdot-}$, it generates H_2O_2, which is subsequently scavenged by CAT and APX. The lower activity of antioxidative enzymes reduces effective ROS scavenging and ROS accumulate in transgenic plants (Figs. 5, 6). DCMU treatment also indicated that the transgenic plants suffered from severe oxidative stress. ROS such as $O_2^{\cdot-}$ and H_2O_2 have also been implicated as age-associated factors that trigger leaf senescence which in turn enhances membrane lipid peroxidation [50]. There was detectable, but not significant, accumulation of MDA in transgenic plants (Fig. 3F). It is possible that the transgenic plants were still undergoing vegetative growth, which prevented the membrane lipid peroxidation.

Liu *et al. Biol Res* (2016) 49:30

Page 9 of 15
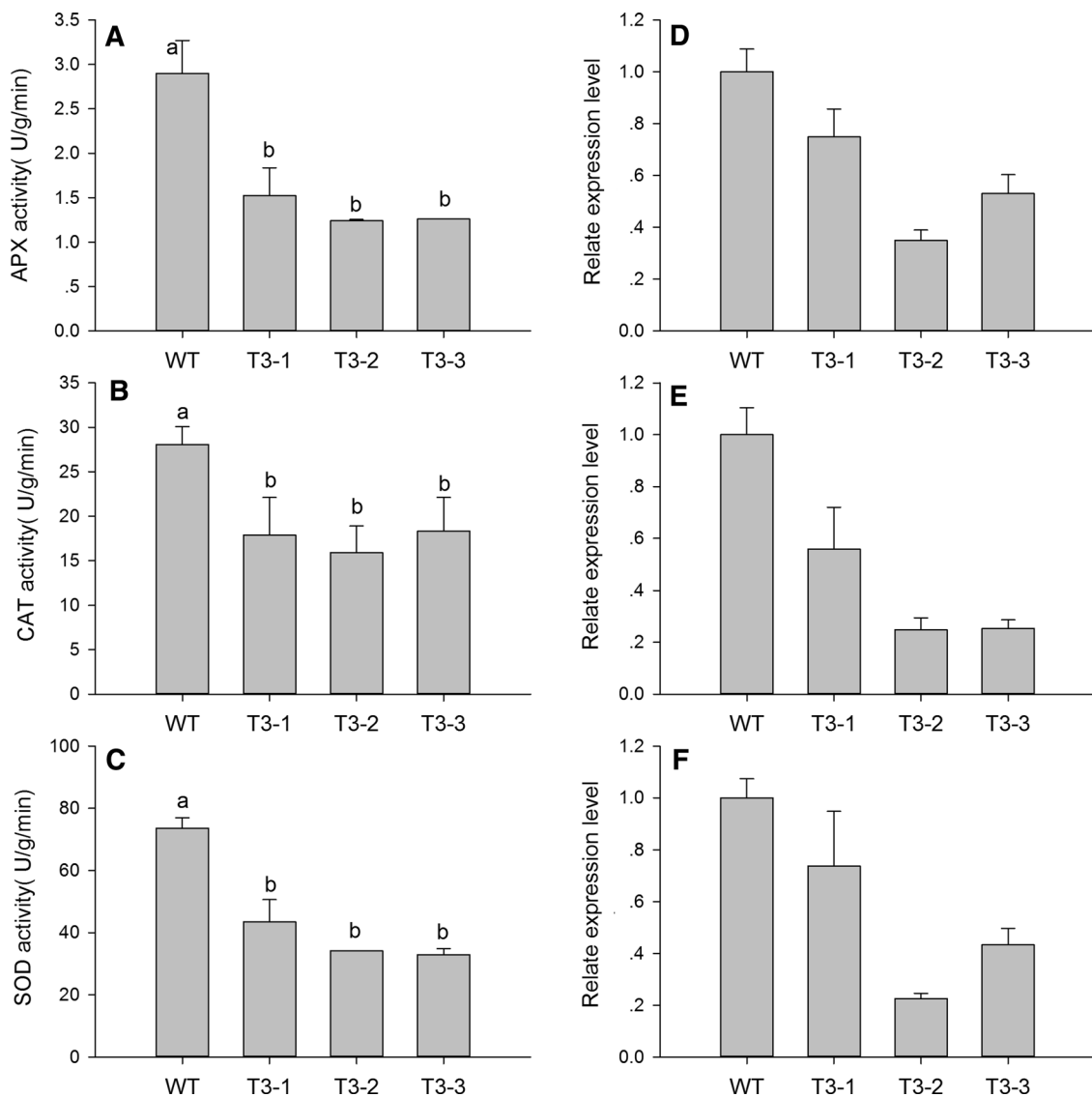
Fig. 6 Activity and expression analysis of antioxidant enzymes in the WT, T3-1, T3-2, and T3-3 tobacco plants. **A** and **D** represent ascorbate peroxidase (APX), **B** and **E** represent catalase (CAT), and **C** and **F** represent superoxide dismutase (SOD). 18S RNA (GenBank Accession Number: AJ236016) was used as a housekeeping gene. The gene names and primers used for qRT-PCR analysis are presented in Additional file 6. Five biological replicates were used for each *line* to study of antioxidant enzyme activity. The standard error of the mean of three biological replicates (nested within three technical replicates) is represented by the *error bars* in qRT-PCR analysis

Reactive oxygen species (ROS) induced plastid damage; chloroplast ROS influenced leaf senescence, and determined the viability and longevity of green tissues [51]. Downregulated genes are involved in senescence; *CAB* and *RuBisCO* small subunit, are responsible for the regulation of photosynthetic proteins. Chlorophyllase (CHL) operates the chlorophyll degradation pathway. The accumulation of *CHL m*RNA controls the release of ROS from the thylakoid membrane, which then initiates senescence. In addition to the above, relatively lower

leaf water content led to a reduction in water potential, stomatal closure, and lower CO_2 levels in aging mesophyll tissues, thereby reducing the net photosynthetic rate (Fig. 3E; Additional file 5: Fig. S3). The degradation of chlorophyll and photosynthetic proteins in transgenic plants suppressed the net photosynthetic rate (Fig. 3). A decline in photosynthetic capacity is a major feature of senescent leaves. In photosynthetic reactions, photosystem II, photosystem I, cytochrome b6/f complex, photosynthetic electron transport, and F-type ATPase

Liu *et al. Biol Res* (2016) 49:30

Page 10 of 15
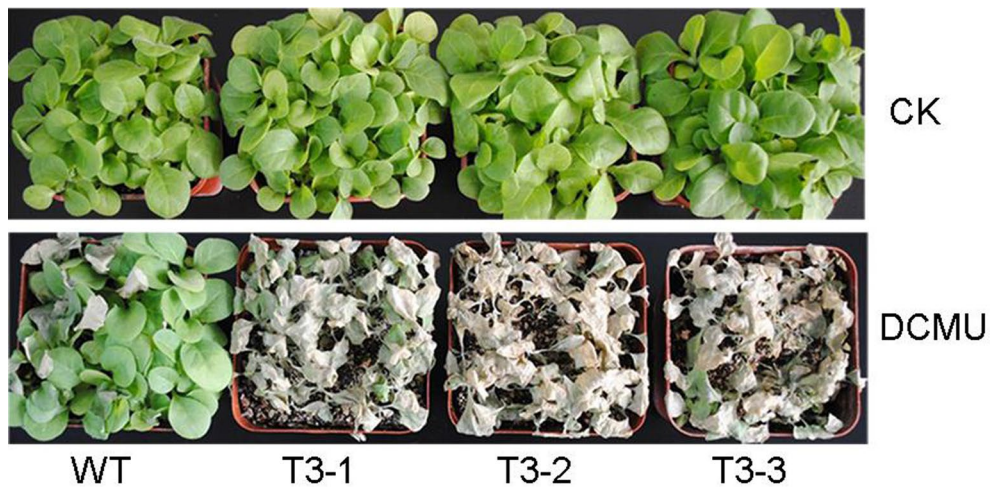
Fig. 7 Enhanced sensitivity of transgenic plants to oxidative stress. The 3-week-old plants were treated with 70 μM DCMU for 10 days
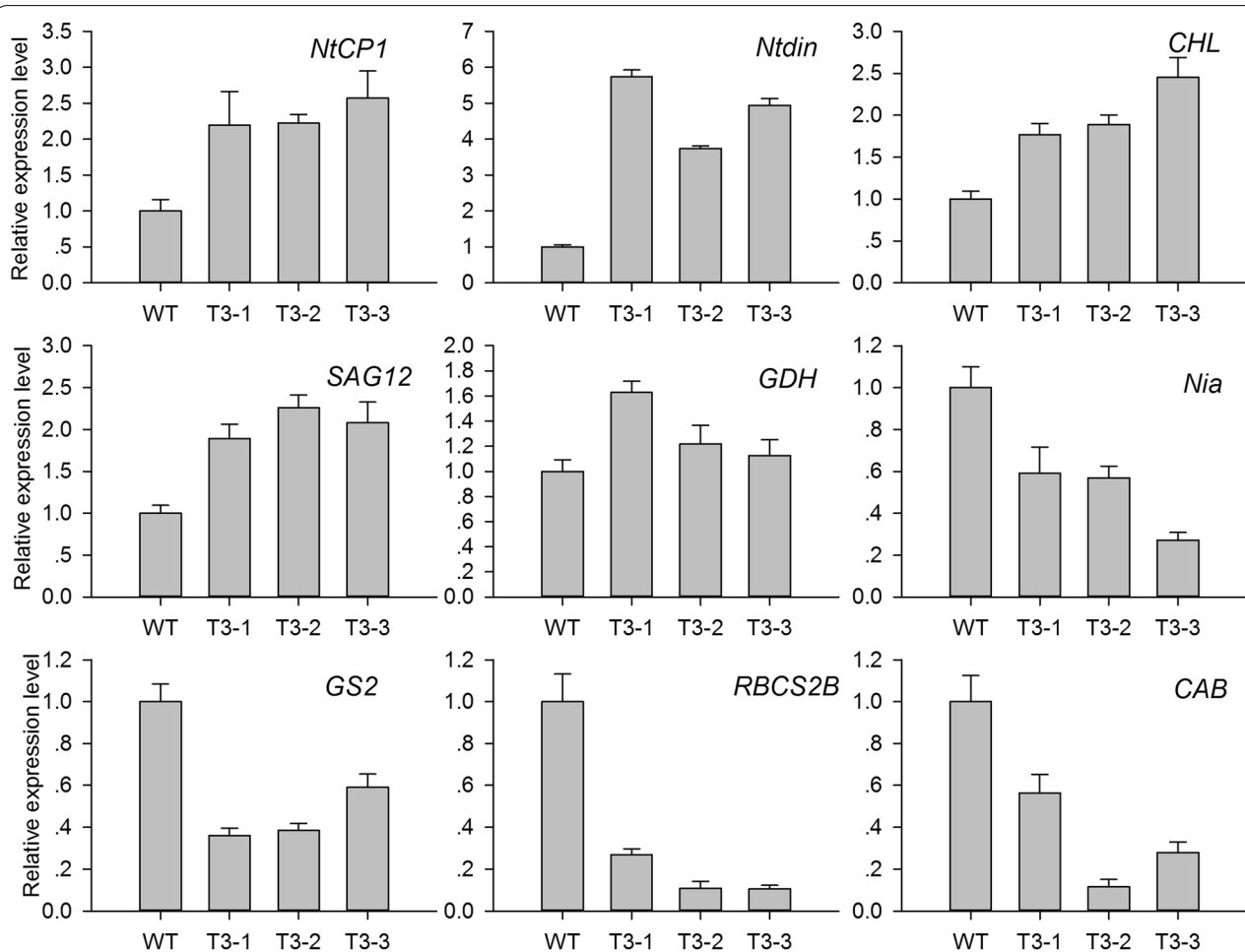
Fig. 8 Expression analysis of senescence marker genes in WT and transgenic plants. *NtCP1* cysteine protease, *SAG12* cysteine protease, *Ntdin* a tobacco senescence-associated gene, *CHL* chlorophyllase, *GDH* glutamate dehydrogenase, *Nia* nitrate reductase, *GS2* chloroplastic glutamine synthetase, *RBCS2B* RuBisCO small subunit, *CAB* chlorophyll *a/b* binding protein. 18S RNA (GenBank Accession Number: AJ236016) was used as housekeeping gene. The gene names and primers used for qRT-PCR analysis are shown in Additional file 6. The standard error of the mean of three biological replicates (nested within three technical replicates) is represented by the *error bars* in qRT-PCR analysis

Liu *et al. Biol Res* (2016) 49:30

Page 11 of 15

distributed 87 downregulated unigenes in transgenic plants (Fig. 4). This further revealed that photosynthesis was suppressed in transgenic plants.

Proteins in plant leaves are constantly engaged in stable turnover. With plant leaf senescence, this dynamic balance is disturbed and leads to protein degradation. Protein degradation generally occurs via the ubiquitin–proteasome system. GO analysis indicated that several ubiquitin-mediated proteolysis unigenes were upregulated in transgenic plants (Additional file 2). In plants, a portion of senescence-associated proteases are localized in senescence-associated vacuoles to degrade chloroplast-derived proteins, including those encoding cysteine proteases, and vacuolar processing enzymes [52, 53]. *NtCP1* is only expressed in senescent tobacco leaves and was not induced in mature green leaves or by abiotic stress. *SAG12*, expressed in mature and senescent leaves, can also be used as a leaf senescence marker in tobacco [54]. Cysteine proteinases (*NtCP1* and *SAG12*) are important for the degradation of photosynthetic proteins such as Rubisco and Rubisco activase [55]. *NtCP1* and *SAG12* were induced indicating that senescence had started in transgenic plants.

We made a preliminary analysis of the effect of leaf senescence on the terpenoid synthesis pathway. Monoterpene production is inhibited under oxidative stress [56]. Monoterpenes, including β-Myrcene and linalool, have lower production in transgenic plants compared to wild-type plants (Fig. 1). In addition, carotenoid biosynthesis had 34 downregulated unigenes, geranylgeranyl reductase and solanesyl diphosphate synthase are downregulated in the MEP pathway (Additional file 3). The release of farnesene can reduce the supply of substrate for other terpenes in the MVA pathway such as caryophyllene and sterols. Sterols are essential for plant development and growth. This may be an additional reason for the senescence phenotype.

Conclusion

The analysis of differentially expressed unigenes, physiological and biochemical parameters related to senescence highlighted that ROS play an important role in the senescence of transgenic plants. This study also indicates that Illumina sequencing technology can be applied as a rapid method for de novo transcriptome analysis of tobacco with unavailable genomic information.

Methods

Plant materials and treatments

Seeds (*Nicotiana tabacum* NC89) of WT, T3-1, T3-2 and T3-3 were germinated on Murashige–Skoog (MS) agar medium, in closed glass dishes for 14 days at 25/20 °C day/night cycle and 16:8 (L:D) h photoperiod.

Seedlings were transplanted into vermiculite and grown at 25–30 °C/20–25 °C (day/night temperature regime) under a 16:8 h photoperiod 300–700 μmol m^{-2} s^{-1} photon flux density (PFD) and 50–60 % relative humidity in a greenhouse. Leaf samples were obtained from 8-week-old plants for subsequent experiments. At 8 weeks, the transgenic plants are still in vegetative growth. So the plants were considered to be at similar developmental stages. The measurements of physiological and biochemical parameters were conducted on the youngest fully expanded leaves. Five biological repeats were used in physiological and biochemical experiments.

For reagent treatment, seeds of WT, T3-1, T3-2 and T3-3 were sown into vermiculite and grown in an illuminated incubation chamber (GXZ-260C). Three week-old WT and transgenic plants were sprayed with 70 μM 3-(3,4-dichlorfenyl)-1,1-dimethylkarbonyldiamid (DCMU).

Transformation and identification of transgenic tobacco plants

Based on the cDNA sequence of *MdAFS1* (GenBank accession number AY182241), a specific primer was designed (Additional file 6). Total RNA was isolated from apple peel of '*white winter pearmain*' using Trizol (Tiangen, Beijing, China). DNA-free total RNA was reverse-transcribed using a RevertAid First-strand cDNA Synthesis Kit (MBI Fermentas, Beijing, China) according to the manufacturer's protocol. The *MdAFS1* gene was isolated from apple (*white winter pearmain*). The open reading frame (ORF) of *MdAFS1* cDNA was inserted into the pBI122 expression vector under the control of the 35S Cauliflower mosaic virus promoter. The 35S-*MdAFS1* plasmid was introduced into *Agrobacterium tumefaciens* LBA4404, and was verified by PCR and sequencing. *N. tabacum* (NC89, saved by the current laboratory) was transformed with the resultant plasmid using the standard *Agrobacterium-* mediated method [57]. Three independent third generations lines (T3-1, T3-2, T3-3) were selected for further experimentation.

Samples and analytical conditions for GC–MS analysis

Each 1.0 g fresh tobacco flower sample was extracted with 6 ml of extraction buffer supplemented with 50 mM KCl and 10 mM MgCl$_2$ in a sealed container [58, 59]. The volatile compounds were collected with solid-phase microextraction (SPME) for 40 min at 40 °C.

Volatile compound analysis was performed with GCMS-QP2010 with a FID detector (Shimadzu, Tokyo, Japan). A Rtx-5MS fused-silica column (30 m × 0.32 mm × 0.25 μm) was used. The oven temperature was initially held for 2 min at 35 °C, ramped at 6 °C/min up to 120, 10 °C/min up to 180 and 20 °C/min

Liu *et al. Biol Res (2016) 49:30*

Page 12 of 15

up to 230 °C. Split injection (5:1) was used. The carrier gas was helium with a flow rate of 2.2 ml/min. Injector and FID detector temperature were held at 250 and 280 °C, respectively.

Qualitative method The results were analyzed using standard NIST08 gallery and spectra.

Quantitative method The results were analyzed using the normalization of peak area method.

Measurement of pigment content

Pigment was extracted from fresh leaf samples ($\approx$0.1 g) using 80 % acetone at room temperature in darkness until the leaf tissue was completely bleached. The extract was centrifuged at 5000g for 5 min, and the supernatant was collected and used in spectrophotometric analysis with a spectrophotometer (UV-1780, Shimadzu, Tokyo, Japan) at an absorbance wavelength of 470, 646 and 663 nm. The chlorophyll concentration was calculated using the following formula: chlorophyll a (C_a) = 12.21*A_{663} − 2.81*A_{646}; and chlorophyll b (C_b) = 20.13*A_{646} − 5.03*A_{663}. The total chlorophyll (a + b) content (mg g^{-1} FW) was then calculated. The carotenoid concentration (C_{x*c}) was calculated using the following formula: carotenoids = (1000*A_{470} − 3.27*C_a − 104*C_b)/229.

Photosynthetic gas exchange measurements

CO_2 gas exchange was measured between 9:00 and 11:00 h on the same day using a portable photosynthesis system (CIRAS-2, PP Systems, Herts, UK). Experiments were performed under the following conditions: greenhouse temperature (25 ± 1 °C); CO_2 concentration, 390 μl l^{-1}; PFD, 1200 μmol m^{-2} s^{-1}, and relative humidity, 70–80 %. Irradiance was controlled by the automatic control function of the CIRAS-2 photosynthetic system.

Physiological assays for leaf senescence

Each 0.5 g leaf sample was homogenized in 5 ml of 50 mM sodium phosphate buffer (pH 7.8) supplemented with 1 mM EDTA and 2 % (w/v) polyvinylpyrrolidone (PVP). The homogenate was centrifuged at 12,000g for 20 min at 4 °C; the supernatant was immediately used for the determination of O_2^- radical production rate, soluble protein content, and antioxidant enzyme activities. All assays were performed at 4 °C. Superoxide dismutase (SOD), catalase (CAT), and ascorbate peroxidase (APX) activities were determined as previously described [60]. Total soluble protein content was determined according to Bradford using bovine serum albumin (BSA) as the standard [61]. The assay for O_2^- content was conducted as described by Yang [62].

H_2O_2 content was measured according to Gay and Gebicki [63]. Tobacco leaves (0.5 g) were ground with

liquid nitrogen, then transferred to a centrifuge tube, to which 2 ml of cold acetone was added. After centrifugation at 10,000g for 10 min, 1 ml of supernatant and 3 ml of 20 % titanium tetrachloride ($TiCl_4$) were centrifuged at 4000g for 15 min. Twenty percentage (v/v) H_2SO_4 was added to the precipitate, dissolved, and the absorbance was determined at 410 nm.

Lipid peroxidation was determined by estimating malondialdehyde (MDA) content [64]. A 10 % solution of trichloroacetic acid (TCA) containing 0.6 % 2-thiobarbituric acid (TBA) and heated at 95 °C for 15 min, and the absorbances were determined at 450, 532 and 600 nm. All spectrophotometric analyses were performed using a spectrophotometer (UV-1780, Shimadzu, Tokyo, Japan).

Water content and seed biomass were determined using a drying oven (Yiheng, Shanghai, China). Fresh leaf samples were dried at 105 °C for 30 min, and 60 °C for 48 h. After collection, seeds were heated at 35 °C to constant weight, and the tobacco seeds were used in biomass statistics.

Histochemical staining of H_2O_2 and O_2^-

H_2O_2 and O_2^- accumulations were detected using 3,3′-diaminobenzidine (DAB) and nitroblue tetrazolium (NBT) staining methods [65, 66], respectively. H_2O_2 reacts with DAB to form a reddish-brown stain. Tobacco leaf discs (1.4 cm diameter) were incubated in 1 mg/ml DAB solution in the dark at room temperature for 16 h. Leaf discs were boiled in ethanol (95 %) for 10 min and then cooled to room temperature. The leaf discs were then extracted with fresh ethanol and photographed. O_2^- reacts with NBT to form a blue stain. A 0.5 mg/ml NBT solution was used in this experiment. The procedure used was similar to H_2O_2 staining.

Transcriptome analysis

The tobacco plants were grown under greenhouse conditions as described previously. Samples were collected from 8-week-old plants. To produce a transcriptome dataset with a wide coverage, RNA was extracted from pooled samples of leaves from four plants of WT and T3-2, respectively. The high-quality reads were assembled with the software package Velvet_1.2.10. The trimmed Solexa transcriptome reads were mapped onto the unique consensus sequences using Bowtie. Unigenes were compared to records in public databases, including the National Center for Biotechnology Information (NCBI, 2013), SWISS-PROT, kyoto encyclopedia of genes and genomes database (KEGG), and gene ontology (GO). Transcriptome sequencing was performed by Capital Bio Corporation (Beijing, China), using Hiseq 2000.

Liu *et al. Biol Res* (2016) 49:30

Page 13 of 15

qRT-PCR analysis

Sampling from 8-week-old plants under the same greenhouse conditions as previously described, qRT-PCR analysis was conducted according to the MIQE guidelines [67, 68]. Total RNA was isolated using a total RNA isolation system (Tiangen, Beijing, China). First-strand cDNAs were synthesized using a First-strand cDNA Synthesis Kit (Tiangen, Beijing, China). qRT-PCR was performed on a Bio-Rad CFX96TM Real-time PCR System using SYBR Real Master Mix (Transgen, Beijing, China) using the following PCR thermal cycle conditions: predenaturation at 95 °C for 30 s; followed by 40 cycles of 95 °C for 5 s, 60 °C for 15 s, and 72 °C for 20 s. 18S RNA (GenBank Accession Number: AJ236016) was used as housekeeping gene. Three biological replicates were performed for each line, and the standard curve method was used for statistical analysis.

Statistical analysis

Statistical analyses were performed using SigmaPlot 12.0 software, Excel, and data processing system (DPS) procedures (Zhejiang University, Zhejiang, China). Differences among means were compared using Tukey's multiple range test at a 0.05 probability level.

Additional files

Additional file 1: Fig. S1. Validation of transcript levels of six candidate unigenes of the transcriptome by qRT-PCR. Upregulated unigenes of the transcriptome database: Locus_72229: *Nicotiana tabacum* glycine-rich protein precursor, Locus_4438: Ent-copalyl diphosphate synthase, Locus_712: Polyphenol oxidase; downregulated unigenes of the transcriptome database: Locus_10435: Inositol-3-phosphate synthase, Locus_5382: Ethylene-responsive transcription factor 5, Locus_93559: Calvin cycle protein. The gene names and primers used for qRT-PCR analysis are shown in Additional file. 1. The standard error of the mean of three biological replicates (nested within three technical replicates) is represented by error bars.

Additional file 2. Differentially expressed and identified unigenes in photosynthesis, nitrogen metabolism, nutrient reservoir activity, antioxidant activity, ubiquitin-mediated proteolysis, cell growth, and death.

Additional file 3. Differentially expressed and identified unigenes in secondary metabolism signaling pathways.

Additional file 4: Fig. S2. Antioxidant metabolite levels of the WT and transgenic plants.

Additional file 5: Fig. S3. The relative values of GS, Pn, Ci, in tobacco leaves.

Additional file 6. List of primers used for qRT-PCR analysis.

Abbreviations

APX: ascorbate peroxidase; CAB: chlorophyll *a/b* binding protein; CAT: catalase; CHL: chlorophyllase; DAB: 3,3′-diaminobenzidine; GDH: glutamate dehydrogenase; GO: gene ontology; GS2: chloroplastic glutamine synthetase; GC/MS: gas chromatography–mass spectrometry; H_2O_2: hydrogen peroxide; KEGG: kyoto encyclopedia of genes and genomes; LSD: leaf senescence database; MDA: malondialdehyde; MS: Murashige–Skoog; NBT: nitroblue tetrazolium; Nia: nitrate reductase; NtCP1: cysteine protease; Ntdin: a tobacco senescence-associated gene; O_2^-: superoxide anion; POD: peroxidase; qRT-PCR: quantitative real time-polymerase chain reaction; RBCS2B: RuBisCO small subunit; ROS: reactive oxygen species; SAG12: cysteine protease; SOD: superoxide dismutase; WT: wild-type.

Authors' contributions
YHZ and YL designed the research study; YL, HL, RRZ, BL, and LW conducted the study, YL and QJF analyzed the data, and YL wrote the manuscript. All authors read and approved the final manuscript.

Author details
[1] State Key Laboratory of Crop Biology, College of Life Sciences, Shandong Agricultural University, 61 Dai Zong Street, Tai'an 271018, Shandong, People's Republic of China. [2] Shandong Institute of Pomology, 66 Long Tan Road, Tai'an 271018, Shandong, People's Republic of China.

Competing interests
The authors declare that they have no competing interests. Compliance with ethical guidelines. This article does not contain any studies with human or animal subjects performed by any of the authors.

References

1. Kännaste A, Vongvanich N, Borg-Karlson AK. Infestation by a *Nalepella* species induces emissions of α-and β-farnesenes,(−)-linalool and aromatic compounds in Norway spruce clones of different susceptibility to the large pine weevil. Arthropod-Plant Interact. 2008;2(1):31–41.
2. Bengtsson M, Bäckman AC, Liblikas I, et al. Plant odor analysis of apple: antennal response of codling moth females to apple volatiles during phenological development. J Agric Food Chem. 2001;49(8):3736–41.
3. Bain JM, Mercer FV. The Submicroscopio Cytology of Superficial Scald, a Physiological Disease of Apples. Aust J Biol Sci. 1963;16(2):442–9.
4. Meigh DF. Volatile compounds produced by apples. I.—Aldehydes and ketones. J Sci Food Agric. 1956;7(6):396–411.
5. Whitaker BD, Solomos T, Harrison DJ. Quantification of α-farnesene and its conjugated trienol oxidation products from apple peel by C18-HPLC with UV detection. J Agric Food Chem. 1997;45(3):760–5.
6. Zubini P, Baraldi E, De Santis A, et al. Expression of anti-oxidant enzyme genes in scald-resistant 'Belfort' and scald-susceptible 'Granny Smith' apples during cold storage. J Hortic Sci Biotechnol. 2007;82(1):149–55.
7. Lange BM, Rujan T, Martin W, et al. Isoprenoid biosynthesis: the evolution of two ancient and distinct pathways across genomes. Proc Natl Acad Sci USA. 2000;97(24):13172–7.
8. Lombard J, Moreira D. Origins and early evolution of the mevalonate pathway of isoprenoid biosynthesis in the three domains of life. Mol Biol Evol. 2011;28(1):87–99.
9. Pechous SW, Whitaker BD. Cloning and functional expression of an (E, E)-α-farnesene synthase cDNA from peel tissue of apple fruit. Planta. 2004;219(1):84–94.
10. Suzuki M, Kamide Y, Nagata N, et al. Loss of function of 3-hydroxy-3-methylglutaryl coenzyme A reductase 1 (HMG1) in Arabidopsis leads to dwarfing, early senescence and male sterility, and reduced sterol levels. Plant J. 2004;37(5):750–61.
11. Keim V, Manzano D, Fernández FJ, et al. Characterization of Arabidopsis FPS isozymes and FPS gene expression analysis provide insight into the biosynthesis of isoprenoid precursors in seeds. PLoS One. 2012;7(11):e49109.
12. Masferrer A, Arró M, Manzano D, et al. Overexpression of Arabidopsis thaliana farnesyl diphosphate synthase (FPS1S) in transgenic Arabidopsis induces a cell death/senescence-like response and reduced cytokinin levels. Plant J. 2002;30(2):123–32.

Liu *et al. Biol Res* (2016) 49:30

Page 14 of 15

13. Bhatia V, Maisnam J, Jain A, et al. Aphid-repellent pheromone E-β-farnesene is generated in transgenic Arabidopsis thaliana over-expressing farnesyl diphosphate synthase2. Ann Bot. 2015;115:581–91.

14. Richter A, Seidl-Adams I, Köllner TG, et al. A small, differentially regulated family of farnesyl diphosphate synthases in maize (*Zea mays*) provides farnesyl diphosphate for the biosynthesis of herbivore-induced sesquiterpenes. Planta. 2015;241(6):1351–61.

15. Huang M, Sanchez-Moreiras AM, Abel C, et al. The major volatile organic compound emitted from Arabidopsis thaliana flowers, the sesquiterpene (E)-β-caryophyllene, is a defense against a bacterial pathogen. New Phytol. 2012;193(4):997–1008.

16. Kempinski C, Jiang Z, Bell S, Chappell J. Metabolic engineering of higher plants and algae for isoprenoid production. Adv Biochem Eng Biotechnol. 2015;148:161–99.

17. De Ford C, Ulloa JL, Catalán CAN, et al. The sesquiterpene lactone polymatin B from *Smallanthus sonchifolius* induces different cell death mechanisms in three cancer cell lines. Phytochemistry. 2015;117:332–9.

18. Rodriguez-Concepción M, Boronat A. Elucidation of the methylerythritol phosphate pathway for isoprenoid biosynthesis in bacteria and plastids: a metabolic milestone achieved through genomics. Plant Physiol. 2002;130:1079–89.

19. Dudareva N, Andersson S, Orlova I, et al. The nonmevalonate pathway supports both monoterpene and sesquiterpene formation in snapdragon flowers. Proc Natl Acad Sci USA. 2005;102(3):933–8.

20. Xing S, Miao J, Li S, et al. Disruption of the 1-deoxy-D-xylulose-5-phosphate reductoisomerase (DXR) gene results in albino, dwarf and defects in trichome initiation and stomata closure in Arabidopsis. Cell Res. 2010;20(6):688–700.

21. Kishimoto K, Matsui K, Ozawa R, et al. Analysis of defensive responses activated by volatile allo-ocimene treatment in *Arabidopsis thaliana*. Phytochemistry. 2006;67(14):1520–9.

22. Yamasaki Y, Kunoh H, Yamamoto H, et al. Biological roles of monoterpene volatiles derived from rough lemon (Citrus jambhiri Lush) in citrus defense. J Gen Plant Pathol. 2007;73(3):168–79.

23. Chaimovitsh D, Abu-Abied M, Belausov E, et al. Microtubules are an intracellular target of the plant terpene citral. Plant J. 2010;61(3):399–408.

24. Rogers HJ. Is there an important role for reactive oxygen species and redox regulation during floral senescence? Plant Cell Environ. 2012;35(2):217–33.

25. Tewari RK, Watanabe D, Watanabe M. Chloroplastic NADPH oxidase-like activity-mediated perpetual hydrogen peroxide generation in the chloroplast induces apoptotic-like death of *Brassica napus* leaf protoplasts. Planta. 2012;235(1):99–110.

26. Van Breusegem F, Dat JF. Reactive oxygen species in plant cell death. Plant Physiol. 2006;141(2):384–90.

27. Kangasjärvi S, Neukermans J, Li S, et al. Photosynthesis, photorespiration, and light signalling in defence responses. J Exp Bot. 2012;63:1619–36.

28. Girondé A, Poret M, Etienne P, et al. A profiling approach of the natural variability of foliar N remobilization at the rosette stage gives clues to understand the limiting processes involved in the low N use efficiency of winter oilseed rape. J Exp Bot. 2015;66(9):2461–73.

29. Quirino BF, Noh YS, Himelblau E, et al. Molecular aspects of leaf senescence. Trends Plant Sci. 2000;5(7):278–82.

30. Lin CR, Lee KW, Chen CY, et al. SnRK1A-interacting negative regulators modulate the nutrient starvation signaling sensor SnRK1 in source-sink communication in cereal seedlings under abiotic stress. Plant Cell. 2014;26(2):808–27.

31. Schippers JHM, Schmidt R, Wagstaff C, et al. Living to die and dying to live: the survival strategy behind leaf senescence. Plant Physiol. 2015;169(2):914–30.

32. Wingler A, Purdy S, MacLean JA, et al. The role of sugars in integrating environmental signals during the regulation of leaf senescence. J Exp Bot. 2006;57(2):391–9.

33. Hörtensteiner S, Feller U. Nitrogen metabolism and remobilization during senescence. J Exp Bot. 2002;53(370):927–37.

34. Lin JF, Wu SH. Molecular events in senescing Arabidopsis leaves. Plant J. 2004;39(4):612–28.

35. Zavaleta-Mancera HA, Thomas BJ, Thomas H, et al. Regreening of senescent Nicotiana leaves II. Redifferentiation of plastids. J Exp Bot. 1999;50(340):1683–9.

36. Gan S, Amasino RM. Inhibition of leaf senescence by autoregulated production of cytokinin. Science. 1995;270(5244):1986–8.

37. Himelblau E, Amasino RM. Nutrients mobilized from leaves of *Arabidopsis thaliana* during leaf senescence. J Plant Physiol. 2001;158(10):1317–23.

38. Bazargani MM, Sarhadi E, Bushehri AAS, et al. A proteomics view on the role of drought-induced senescence and oxidative stress defense in enhanced stem reserves remobilization in wheat. J Proteomics. 2011;74(10):1959–73.

39. Schwachtje J, Minchin PEH, Jahnke S, et al. SNF1-related kinases allow plants to tolerate herbivory by allocating carbon to roots[J]. Proc Natl Acad Sci. 2006;103(34):12935–40.

40. Gregersen PL, Culetic A, Boschian L, et al. Plant senescence and crop productivity. Plant Mol Biol. 2013;82(6):603–22.

41. Palenchar PM, Kouranov A, Lejay LV, et al. Genome-wide patterns of carbon and nitrogen regulation of gene expression validate the combined carbon and nitrogen (CN)-signaling hypothesis in plants. Genome Biol. 2004;5(11):R91.

42. Aoyama S, Reyes TH, Guglielminetti L, et al. Ubiquitin ligase ATL31 functions in leaf senescence in response to the balance between atmospheric CO2 and nitrogen availability in Arabidopsis. Plant Cell Physiol. 2014;55:293–305.

43. Rolland F, Moore B, Sheen J. Sugar sensing and signaling in plants. Plant Cell. 2002;14(Suppl 1):S185–205.

44. Dai N, Schaffer A, Petreikov M, et al. Overexpression of Arabidopsis hexokinase in tomato plants inhibits growth, reduces photosynthesis, and induces rapid senescence. Plant Cell. 1999;11(7):1253–66.

45. Moore B, Zhou L, Rolland F, et al. Role of the Arabidopsis glucose sensor HXK1 in nutrient, light, and hormonal signaling. Science. 2003;300(5617):332–6.

46. Pageau K, Reisdorf-Cren M, Morot-Gaudry JF, et al. The two senescence-related markers, GS1 (cytosolic glutamine synthetase) and GDH (glutamate dehydrogenase), involved in nitrogen mobilization, are differentially regulated during pathogen attack and by stress hormones and reactive oxygen species in *Nicotiana tabacum* L. leaves. J Exp Bot. 2006;57(3):547–57.

47. Tewari RK, Singh PK, Watanabe M. The spatial patterns of oxidative stress indicators co-locate with early signs of natural senescence in maize leaves. Acta Physiol Plant. 2013;35(3):949–57.

48. Gill SS, Tuteja N. Reactive oxygen species and antioxidant machinery in abiotic stress tolerance in crop plants. Plant Physiol Biochem. 2010;48:909–30.

49. Sharma P, Jha AB, Dubey RS, et al. Reactive oxygen species, oxidative damage, and antioxidative defense mechanism in plants under stressful conditions. J Bot. 2012;26.

50. Khanna-Chopra R. Leaf senescence and abiotic stresses share reactive oxygen species-mediated chloroplast degradation. Protoplasma. 2012;249(3):469–81.

51. van Doorn WG, Yoshimoto K. Role of chloroplasts and other plastids in ageing and death of plants and animals: a tale of Vishnu and Shiva. Ageing Res Rev. 2010;9(2):117–30.

52. Guo Y, Cai Z, Gan S. Transcriptome of Arabidopsis leaf senescence. Plant, Cell Environ. 2004;27(5):521–49.

53. Carrión CA, Costa ML, Martínez DE, Mohr C, Humbeck K, Guiamet JJ. In vivo inhibition of cysteine proteases provides evidence for the involvement of 'senescence-associated vacuoles' in chloroplast protein degradation during dark-induced senescence of tobacco leaves. J Exp Bot. 2013;64:4967–80.

54. Beyene G, Foyer CH, Kunert KJ. Two new cysteine proteinases with specific expression patterns in mature and senescent tobacco (*Nicotiana tabacum* L.) leaves. J Exp Bot. 2006;57(6):1431–43.

55. Prins A, Van Heerden PD, Olmos E, Kunert KJ, Foyer CH. Cysteine proteinases regulate chloroplast protein content and composition in tobacco leaves: a model for dynamic interactions with ribulose-1, 5-bisphosphate carboxylase/oxygenase (Rubisco) vesicular bodies. J Exp Bot. 2008;59(7):1935–50.

56. Peñuelas J, Munné-Bosch S. Isoprenoids: an evolutionary pool for photoprotection. Trends Plant Sci. 2005;10(4):166–9.

57. Luo K, Zheng X, Chen Y, et al. The maize Knotted1 gene is an effective positive selectable marker gene for Agrobacterium-mediated tobacco transformation. Plant Cell Rep. 2006;25(5):403–9.

Liu *et al. Biol Res* (2016) 49:30

Page 15 of 15

58. Green S, Friel EN, Matich A, et al. Unusual features of a recombinant apple α-farnesene synthase. Phytochemistry. 2007;68(2):176–88.
59. Green S, Squire CJ, Nieuwenhuizen NJ, et al. Defining the potassium binding region in an apple terpene synthase. J Biol Chem. 2009;284(13):8661–9.
60. Türkan İ, Bor M, Özdemir F, et al. Differential responses of lipid peroxidation and antioxidants in the leaves of drought-tolerant *P. acutifolius* Gray and drought-sensitive *P. vulgaris* L. subjected to polyethylene glycol mediated water stress. Plant Sci. 2005;168(1):223–31.
61. Noble JE, Bailey MJA. Quantitation of protein. Method Enzymol. 2009;463:73–95.
62. Yang S, Tang XF, Ma NN, et al. Heterology expression of the sweet pepper CBF3 gene confers elevated tolerance to chilling stress in transgenic tobacco. J Plant Physiol. 2011;168(15):1804–12.
63. Gay C, Gebicki JM. A critical evaluation of the effect of sorbitol on the ferric–xylenol orange hydroperoxide assay. Anal Biochem. 2000;284(2):217–20.
64. Rao KVM. Sresty TVS. Antioxidative parameters in the seedlings of pigeonpea (*Cajanus cajan* (L.) Millspaugh) in response to Zn and Ni stresses. Plant Sci. 2000;157(1):113–28.
65. Thordal-Christensen H, Zhang Z, Wei Y, Collinge DB. Subcellular localization of H_2O_2 in plants. H_2O_2 accumulation in papillae and hypersensitive response during the barley—powdery mildew interaction. Plant J. 1997;11(6):1187–94.
66. Cai G, Wang G, Wang L, et al. ZmMKK1, a novel group A mitogen-activated protein kinase kinase gene in maize, conferred chilling stress tolerance and was involved in pathogen defense in transgenic tobacco. Plant Sci. 2014;214:57–73.
67. Bustin SA, Benes V, Garson JA, et al. The MIQE guidelines: minimum information for publication of quantitative real-time PCR experiments. Clin Chem. 2009;55(4):611–22.
68. Bustin SA, Beaulieu JF, Huggett J, et al. MIQE precis: practical implementation of minimum standard guidelines for fluorescence-based quantitative real-time PCR experiments. BMC Mol Biol. 2010;11(1):74.